Structure and division of the Golgi complex in *Trichomonas vaginalis* and *Tritrichomonas foetus*

Marlene Benchimol[1)a, b], Karla Consort Ribeiro[a, c], Rafael Meyer Mariante[a], John F. Alderete[d]

[a] Universidade Santa Úrsula, Rio de Janeiro/Brazil
[b] Instituto de Biofísica Carlos Chagas Filho, Universidade Federal do Rio de Janeiro, Rio de Janeiro/Brazil
[c] Programa de pós-graduação em Ciências Morfológicas, Universidade Federal do Rio de Janeiro, Rio de Janeiro/Brazil
[d] Department of Microbiology, University of Texas Health Science Center, San Antonio, TX/USA

Received December 15, 2000
Received in revised version April 12, 2001
Accepted May 28, 2001

Trichomonas vaginalis – Tritrichomonas foetus – Golgi – division – structure

We present observations on the fine structure and the division process of the Golgi complex in the protists *Trichomonas vaginalis* and *Tritrichomonas foetus*, parasites of the urogenital tract of humans and cattle, respectively. The Golgi in trichomonads is a prominent structure, associated with striated parabasal filaments to which this organelle seems to be connected. We followed by immunofluorescence and electron microscopy the Golgi in interphasic and mitotic cells. Ultrastructural studies were performed using fast-freezing fixation, immunocytochemistry using antisera to the known adhesins AP65 and AP51, cytochemistry (acid phosphatase, Ca^{++}-ATPase, zinc iodide-osmium tetroxide technique (ZIO), for analysis of distribution of the endoplasmic reticulum and Golgi complex, and Thiéry's techniques), routine and serial thin-sections. Three-dimensional reconstruction, NBD-ceramide, fluorescent lectin (WGA) and nocodazole treatments were also used. We demonstrate that: (*1*) the Golgi in trichomonads is a single-copy organelle; (*2*) presents a fenestrated structure; (*3*) is formed by 8–12 saccules; (*4*) is connected to the parabasal filaments by thin filamentous bridges; (*5*) by cytochemistry, presents a positive reaction for the lectin WGA, Ca^{++}-ATPase, acid phosphatase, ZIO and Thiéry's techniques; (*6*) does not appear to break down at any point of the cell cycle; (*7*) elongates during the cell cycle by lateral growth; (*8*) is labeled by anti-glutamylated tubulin antibodies, but it is not fragmented by nocodazole treatment; (*9*) before mitosis, the already elongated Golgi ribbon undergoes progressive medial fission, cisternae by cisternae, starting at the cisternae adjacent to the cell surface and ending with the cis-most cisternae; (*10*) the Golgikinesis originates two small Golgi ribbons; (*11*) the Golgi is intensely labeled with the antisera to the AP65 and AP51 adhesins in *T. vaginalis*, thus seeming to be a key station in the production of adhesins.

Introduction

Tritrichomonas foetus and *Trichomonas vaginalis* are flagellated parasitic protists that inhabit the urogenital tract of cattle and humans, respectively. *T. vaginalis* is responsible for trichomonosis, one of the most common sexually transmitted diseases in humans, whereas *T. foetus* often results in reproductive failure and is a cause of significant economic loss throughout the cattle-raising areas of the world. Ultimately, these organisms have been subject of extensive investigation due to *a*) the presence of hydrogenosomes, an anaerobic energy-producing organelle that raises several questions concerning mitochondria evolution and origin of the eukaryotes (Müller, 1993, 1997; Kurland and Andersson, 1999); and to *b*) molecular phylogenetic studies using large and small subunit ribosomal RNAs indicating that these organisms are among the most early diverging eukaryotes (Cavalier-Smith and Chao, 1996; Leipe et al., 1993; Viscogliosi and Brugerolle, 1993) although one cannot discard the possibility of phylogenetic repositioning (Embley and Hirt, 1998).

T. foetus and *T. vaginalis* present a well-developed Golgi complex that is different from several other parasitic protists, like *Giardia, Toxoplasma* and *Trypanosoma*. Although current information shows that the Golgi plays an important role in protein glycosylation, sorting and lysosomes biogenesis, there are few studies on the structure and functions of this organelle in trichomonads (Benchimol and DeSouza, 1985; Queiroz et al., 1991; Morgado and DeSouza, 1998). Due to its prominent size, the Golgi in trichomonads may play an important function, not yet established.

In trichomonads, the Golgi complex corresponds to the Parabasal Apparatus, formed by the Golgi cisternae and the parabasal filaments (Honigberg and Brugerolle, 1990). It is

[1)] Dr. Marlene Benchimol, Rua Jornalista Orlando Dantas, 59, CEP 222–31–010, Botafogo, Rio de Janeiro-RJ/Brazil, e-mail: marleneb@domain:com.br, Fax: +55 21 2553 1615.

0171-9335/01/80/09-593 $15.00/0

dorsally located and to the right of the nucleus consisting of elongated cisternae with dilated rims. The parabasal filament is a microfibrillar strand linked to the basal bodies. Some authors claim that the two parabasal filaments give support to Golgi cisternae and that *T. vaginalis* presents two Golgi complexes (Honigberg and Brugerolle, 1990).

T. foetus and *T. vaginalis* are extracellular parasites and, for infection, they must overcome the mucus barrier and parasitize the vaginal epithelium (Nielsen and Nielsen, 1975; Alderete and Garza, 1988). It is noteworthy that cytoadherence is a prerequisite for cytopathogenicity, and four surface proteins (adhesins) seem to mediate the interaction of *T. vaginalis* with epithelial cells (Alderete and Garza, 1988; Arroyo et al., 1992). The Golgi complex in trichomonads may be involved in the processing of these proteins. Additional studies are necessary to gain better knowledge about this pathogen and to understand the role played by the Golgi and its possible participation during the disease development.

Recently, it was demonstrated by cell fractionation and biochemical analysis that the Golgi complex in *T. foetus* would be the principal site of Ca^{2+} uptake in these cells (Almeida et al. submitted). In this regard, a calcium participation in the process of secretory protein condensation which is postulated to occur in higher eukaryotes (Pozzan et al., 1994) might as well be expected in trichomonads.

Information on Golgi biogenesis is scant, thus studies are necessary to clarify how the Golgi is distributed between the daughter cells during the division process. In higher eukaryotic cells, the Golgi fragments during mitosis and the vesicles are equally distributed to each daughter cell. In the present study we intend to better characterize the ultrastructure of the Golgi complex in trichomonads and also shed some light in the process of Golgi partition in these organisms.

Materials and methods

Cell culture

The K strain of *T. foetus* was isolated by Dr. H. Guida (Embrapa, Rio de Janeiro, Brazil) from the urogenital tract of a bull. *T. vaginalis*, strain JT, was isolated from a patient attending the Rio de Janeiro Federal University Hospital. *T. vaginalis* isolate 347^+ was provided by Dr. Alderete and was also used. The cells were cultivated in TYM Diamond's medium (Diamond, 1957) supplemented with 10% fetal calf serum (*T. foetus*) or 5% horse serum (*T. vaginalis*). Cultures were maintained at 37 °C and subcultured every day.

Immunofluorescence

Cells were centrifuged and washed in warm phosphate-buffered saline (PBS), pH 7.2, and then fixed with 4% paraformaldehyde in 0.1 M cacodylate buffer, pH 7.2. Next, the cells were washed again in PBS and were allowed to adhere to coverslips previously coated with poly-L-lysine. After that, the cells were permeabilized with 2% Nonidet (NP40) at room temperature for 40 minutes and in 100% acetone at −20 °C for 15 minutes. Fixed cells were quenched using 50 mM ammonium chloride solution and 3% bovine serum albumin/PBS. They were then incubated for 3 hours with: (*1*) the individual polyclonal rabbit antisera to the adhesins AP65 and AP51 (Arroyo et al., 1992; Alderete and Garza, 1988), as Golgi markers, and/or (*2*) with the monoclonals anti-alpha-tubulin #357 (Amersham, UK) or #5168 (Sigma Chemical Co., USA), or anti-acetylated alpha-tubulin #6793 (Sigma Chemical Co., USA), followed by incubation for one hour in the dark at room temperature with a rodamine- or fluorescein-conjugated anti-rabbit and/or anti-mouse antibody diluted 1:100 (Sigma, USA). In some experiments the cells were stained with 2 mM DAPI to visualize the nucleus and better determine the Golgi position. The cells were washed in PBS and examined with an Axiophot II Zeiss microscope, equipped with UV epifluorescence. Images were acquired with a Hamamatsu chilled CCD camera C5985. Subsequently, the images were overlaid with DIC images and processed using Adobe Photoshop (Adobe, USA).

C_6-NBD-ceramide fluorescence

The cells were collected by centrifugation, washed in medium without serum, and allowed to adhere to coverslips previously coated with 0.1% poly-L-lysine in PBS. Then, the living cells were incubated in a solution containing 0.9 µl/ml C_6-NBD-ceramide (Molecular Probes Co., USA) and 0.68 µg/ml bovine albumin (Sigma Chem. Co., USA) in TYM medium, pH 7.2, for 10 minutes at 37 °C in the dark. Subsequently, the cells were washed several times in the same medium and incubated again for 20 minutes as described above. The coverslips containing the cells were mounted and observed in a Zeiss confocal laser scanning microscope (Laser 488/LP515).

Transmission electron microscopy (TEM)

Cells were washed three times in PHEM buffer (50 mM $MgCl_2$, 70 mM KCl, 10 mM EGTA, 20 mM Hepes, 60 mM Pipes, pH 6.8) at 37 °C and fixed overnight at room temperature in 2.5% (v/v) glutaraldehyde in 0.1 M cacodylate buffer (pH 7.2); post-fixation was performed in 1% OsO_4 in cacodylate buffer containing 5 mM $CaCl_2$ and 0.8% potassium ferricyanide. Cells were washed, dehydrated in acetone and embedded in Epon. Ultra-thin sections were stained with uranyl acetate and lead citrate and observed in a Jeol 1210 electron microscope.

Three-dimensional reconstruction

Ribbons of 20 golden serial thin sections were collected from the top of the water surface on carbon-backed, formvar-coated 0.5 mm × 2.0 mm slot grids, and stained in aqueous uranyl acetate for 20 min and lead citrate for 5 min. Serial micrographs were taken and printed at a final magnification of × 150000. The nuclear envelope, Golgi, flagella, and other cell components were outlined with distinct colors and each plane was separately traced in a digitizing table (Numonics 2205) into a 3-D reconstruction program: BIGED for IBM PC (Young et al., 1987). The resulting data files consisted of contour outlines representing cross-sections of the objects of interest within the volume. These files were mounted on a fixed axis creating a reconstructed image that could be rotated along the X, Y, and Z axis. The files were then transferred to a Silicon Graphics workstation and the surfaces between planes were generated using the software package SYNU (Synthetic Universe) (Hessler et al., 1992). Selected images were photographed on a Polaroid digital palette film recorder system.

Thiéry's technique (periodic acid-thiosemicarbazide-silver proteinate)

Ultrathin sections of cells, previously fixed in glutaraldehyde and OsO_4 as described above, were collected on gold grids and treated for 20 min with 1% periodic acid. After rinsing in distilled water the sections were incubated for 48–72 h in aqueous solution containing 1% thiosemicarbazide, and 10% acetic acid. After rinsing sequentially with 10, 5, and 1% acetic acid and distilled water, the sections were exposed to 1% silver proteinate for 30 min in the dark, at room temperature. Sections were observed unstained. Controls were performed by omission of the periodic acid step.

Detection of acid phosphatase

Acid phosphatase activity was detected as previously described (Robinson and Karnovsky, 1983; Queiroz et al., 1991), using either lead nitrate or cerium chloride as the capturing agent. Briefly, the cells were fixed in 0.5% (v/v) glutaraldehyde in 0.1 M cacodylate buffer, pH 7.2, for 5 min and incubated for 30 min at 37 °C in a medium containing 3.6 mM β-glycerophosphate, 10 mM $MgCl_2$, 220 mM sucrose, and 3 mM $CeCl_3$ in 50 mM Tris-maleate buffer, pH 5.0. After successive washings, the samples were re-fixed in 2.5% glutaraldehyde and processed for

TEM. Controls were performed with the omission of β-glycerophosphate from the incubation medium.

Ca^{++}-ATPase

The cells were fixed in 0.5% (v/v) glutaraldehyde in 0.1 M cacodylate buffer, pH 7.2, for 5 min and incubated for 30 min at 37 °C in a medium containing 3.0 mM ATP, 10 mM $CaCl_2$, 220 mM sucrose, and 4 mM lead citrate in 250 mM glycine-KOH buffer, pH 9.0. After successive washings, the samples were re-fixed in 2.5% glutaraldehyde and processed for TEM. Controls were performed with the omission of ATP from the incubation medium.

ZIO technique (Zinc iodide-osmium tetroxide technique)

Cells were routinely fixed for TEM and incubated as previously described (Reinecke and Walther, 1978; Benchimol and De Souza, 1985). Briefly, the cells were washed and incubated in the dark for 17 hours at 4 °C in the zinc iodide-osmium tetroxide reagent prepared as follows: 3 g zinc powder and 1 g resublimated iodine were separately suspended in 10 ml distilled water, then mixed, filtered, and mixed with 50 mM Tris buffer (pH 4.5) in a 1:1 ratio. Four parts of this solution was mixed with one part of 2% OsO_4. For control, the cells were incubated for 30 min at room temperature in either 1 mM N-ethylmaleimide or 1 mM dithiothreitol. After incubation, the cells were washed, dehydrated, and embedded in Epon. Thin sections were observed in a Jeol 1210 electron microscopy.

Freeze fracture and freeze substitution

Previously fixed or unfixed specimens were fast-frozen by "slam-freezing" (Cryopress Med. Vac, Inc., St. Louis, MO, USA). A polished copper block was cooled with liquid nitrogen and the specimen was projected in free-fall against the block. Subsequently, specimens were freeze-fractured at −115 °C in a Balzers BAF 300 freeze-etching machine and submitted to shadowing with platinum/carbon at 2×10^{-6} Torr at an angle of 45°. Replicas were recovered in distilled water, cleaned, and examined in a Zeiss 900 transmission electron microscope. Alternatively, living cells were frozen by high pressure in the Balzers high-pressure machine (HPM 010 Balzers Union, Balzers, FL), transferred to liquid nitrogen and then to a mixture of anhydrous acetone containing 2% osmium tetroxide (v/v) at −90 °C in a freeze-substitution unit (Balzers FSU 010). The material was gradually rewarmed during 24 h until room temperature was attained and then embedded in Epon.

Drug treatment

Nocodazole (Sigma, St Louis, USA) was dissolved at 4 mM in DMSO and was further diluted in culture medium. Controls contained only DMSO at corresponding concentrations. Cells were exposed for 1, 12 or 24 h to 10 μM nocodazole. The cells were centrifuged and fixed (without previous washes) in 2.5% glutaraldehyde and processed for immunofluorescence microscopy and TEM as described above.

Measurements

One hundred micrographs from trichomonads were taken from every cell cycle phase, by TEM and fluorescence microscopy, and Golgi measurements were performed (see Fig. 21). The cell cycle phase was established by several criteria, such as axostyle number and position, nucleus shape, and flagella number and position, as previously described (Ribeiro et al., 2000).

Results

General features of trichomonads

We studied *Tritrichomonas foetus* and *Trichomonas vaginalis* during interphase and division by light and electron microscopy. Basically, similar results were obtained in both species. A non-dividing cell (Fig. 1) is characterized by a teardrop or ovoid shape (when in axenic culture) or amoeboid (when in process of adhesion). These flagellated protists have four (*T. foetus*) or five flagella (*T. vaginalis*) but one is recurrent and adheres to the cell membrane towards the posterior tip of the cell. On the uppermost portion of the cell, the basal bodies present several skeletal appendages. Among them, two types of periodic fibers: the widest and longer, called costa, lies beneath the cell membrane supporting the recurrent flagellum. The other ones, which are thinner and shorter, are the parabasal filaments which are believed to support the Golgi complex (Honigberg and Brugerolle, 1990). Surrounding the flagella emergence region, there is a microtubular structure known as pelta. Another structure, the axostyle, is formed by a ribbon of parallel microtubules running from the anterior to posterior region. Hydrogenosomes, anaerobic energy-producing organelles similar to mitochondria, are distributed throughout the cell, although preferentially located lining the axostyle, whereas lysosomes occupy the posterior region of the cell.

During the synthesis phase of the cell cycle, the cell duplicates all the skeletal and organelle constituents, including the microtubule-organizing centers, which are situated beneath one of the basal bodies. At the onset of mitosis (Fig. 2), each duplicated cytoplast, that lies side by side, undergoes progressive migration during the course of the mitotic spindle formation/elongation until the telophase.

Golgi morphology

By electron microscopy, the Golgi is seen as a single and very prominent structure, reaching 6 μm in length and 1 μm in width, anteriorly located, and presenting 8–12 cisternae (Figs. 1, 3), except when the cell is in division (Fig. 2). The luminal space of the saccules is narrow and in the order of 30–35 nm. The distance separating the saccules is in the same order of magnitude and, as a consequence, the Golgi presents a compact appearance (Figs. 1, 3–4). By freeze-fracture the Golgi complex was observed in most cells when the fracture exposed the cytoplasm. The cisternae presented fenestrated membranes (Figs. 3–4). Budding vesicles were also seen at the rims of every saccule (Figs. 3–4, 5). Various types of vesicles were seen associated with it. Small, uncoated 40-nm vesicles were present at lateral edges of the saccules whereas coated vesicles measured about 75 nm (Fig. 5). By high-pressure freezing, followed by freeze-substitution, the overall Golgi characteristics were found as in the routine preparations, except differences in electron densities along the Golgi cisternae, with the medial cisternae presenting a denser content (Fig. 6) and the presence of thin filamentous bridges, connecting the *cis*-most cisternae to the parabasal filament (Fig. 13).

No disturbance of the Golgi was found after nocodazole treatment (Fig. 7). However, by fast-freezing and freeze-substitution, microtubules were seen connecting the Golgi to the plasma membrane (Fig. 8). Using serial thin-sections, a prometaphase Golgi computer 3D reconstruction model was obtained (Fig. 9).

Cytochemistry/immunocytochemistry

Ca^{++}-ATPase was found in the endoplasmic reticulum and in the Golgi saccules, some of them with a more intense labeling (Fig. 10). Reaction product indicative of the presence of acid phosphatase was observed in some Golgi cisternae (Fig. 11) and in lysosomes, which were seen mainly at the posterior region of the cells (Fig. 11). No reaction product was observed when β-

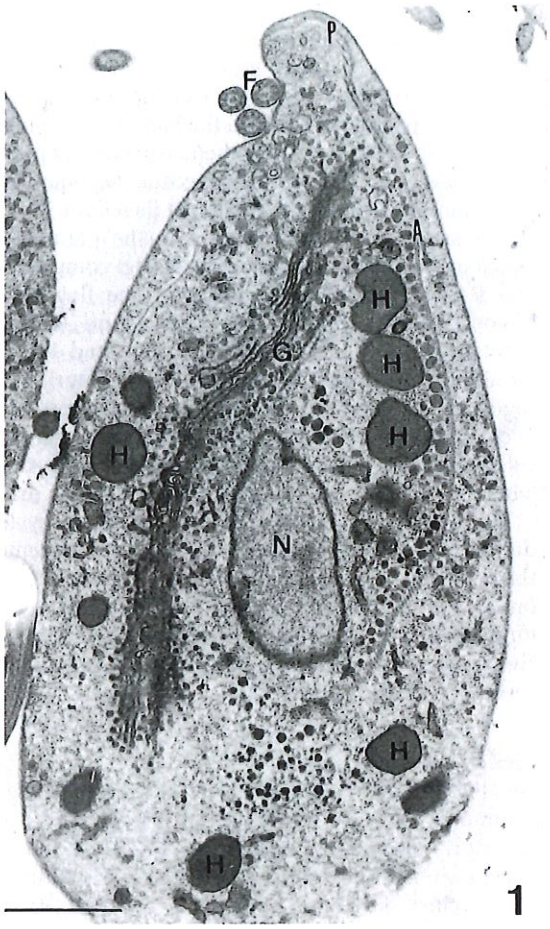

1

2

3

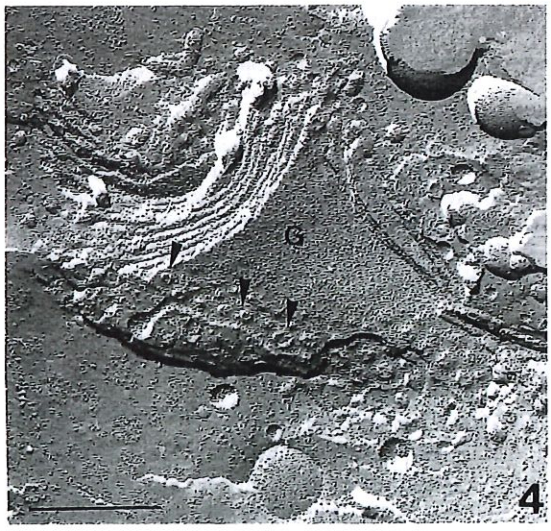

4

◀ **Fig. 1.** General view of *T. foetus* in a longitudinal routine thin section. This cell is in interphase (G1 phase). Note the axostyle (A), three anterior flagella (F), a well-developed Golgi (G) with several budding vesicles, the hydrogenosomes (H), the nucleus (N) and the pelta (P). Bar: 1 μm. **Fig. 2.** General view of *T. foetus* in a longitudinal routine thin section. This cell is at the onset of mitosis: two axostyles (A), two recurrent flagella (RF), two costa (C) and two axostyle tips (*arrowheads* at posterior region) are seen. Note the presence of two small Golgi (G) at the anterior region of the cell. The anterior flagella (F), several hydrogenosomes (H), lysosomes (L) and the nucleus (N) are also seen. Bar: 1 μm. **Fig. 3.** View of freeze-fracture image of *T. foetus* showing the Golgi complex (G). The fracture plane crossed the cytoplasm exposing a prominent Golgi (G) with several lamellae. Hydrogenosomes (H) and profiles of the endoplasmic reticulum (ER) are also seen (Figure 3). **Fig. 4.** Figure 4 shows a close view of the Golgi lamellae with fenestrae (*arrowheads*). Bars: 1 μm (Fig. 3), 0.5 μm (Fig. 4).

glycerophosphate was omitted from the incubation medium (not shown).

Immunogold-labeling using anti-glutamylated tubulin showed an intense decoration of the microtubules in the flagella, axostyle and pelta. However, an intense labeling was also observed on the Golgi (Fig. 12). Other monoclonals antibodies, anti-alpha-tubulin (Fig. 20) or anti-acetylated tubulin were also tested but they did not react with the Golgi.

Golgikinesis

We observed that during the course of the cell cycle the Golgi ribbon seems to elongate (Fig. 21), while maintaining the usual number of cisternae (Fig. 14). After Golgi elongation, reaching 4.7–6.0 μm, the stack underwent progressive medial fission of each cisternae beginning with the one adjacent to the cell surface, ending with the *cis*-most cisternae, near the endoplasmic reticulum (Figs. 14–16). Golgikinesis occurs just before the onset of mitosis, and two small Golgi ribbons, measuring 1.0–1.2 μm each, appear. During the mitotic process each Golgi ribbon migrates together with the anterior portion of each axostyle, positioned between the basal bodies and the nuclear compartment. During the course of mitosis, each ribbon gradually elongates, reaching 3.6 μm at telophase, when each daughter cell presents only one Golgi ribbon. We demonstrated that the Golgi ribbon still elongates during the interphase, reaching a prominent size. Figure 21 shows the progressive Golgi elongation during the course of the cell cycle, obtained after 100 measurements of Golgi in different phases of the cell cycle.

Cytochemistry

Carbohydrate detection was performed using the Thiéry's method, and positive labeling was found on all organellar membranes, Golgi included, and also in the glycogen granules (Fig. 17). Fluorescent WGA was also used as a Golgi marker (not shown) evidencing the presence of N-acetyl-glucosamine residues. By applying the ZIO technique, which allows the analysis of the distribution of the endoplasmic reticulum/Golgi complex system and also the nuclear envelope, these structures were found intensely labeled (Fig. 18). This technique allowed the visualization of the fenestrae in the nuclear envelope and Golgi, and also the interconnections between the cisternae, giving us a different view of the Golgi (Fig. 18).

Golgi biogenesis

In order to follow the Golgi behavior during morphogenesis we took advantage of our previous knowledge of the changes that occur with the nucleus and axostyle, in every cell cycle phase (Ribeiro et al., 2000), and the anti-adhesins antibodies labeling which specifically decorate the secretory pathway, Golgi included, as demonstrated by EM immunocytochemistry (Alderete et al., 2000).

When living cells were examined using C-6-NBD-ceramide, a Golgi marker, and propidium iodide, a nucleus stain, the documentation was not easy due to photobleaching and also the fast cell movement. Therefore, we used fixed cell preparations for fluorescence microscopy to carefully analyze each cell cycle phase. Double labeling was performed using (*1*) anti-tubulin in order to determine the number and position of the axostyles for the identification of the mitotic phase, and (*2*) antisera to adhesins AP65 and AP51 (Figs. 19, 20). In some experiments the nucleus was stained with DAPI to better determine the Golgi position. Similar results were obtained with both *T. foetus* and *T. vaginalis* with all approaches, except with the anti-adhesin antibodies, which labeled only the Golgi of *T. vaginalis*. The Golgi complex was promptly recognized as a characteristic fluorescent structure in the juxtanuclear position.

In interphase cells, only one Golgi was seen (Fig. 19A) whereas two structures were found in those cells in the process of synthesis (Fig. 19B) and division (Fig. 19C–H). Soon after the skeletal structures such as flagella, costa, pelta-axostyle system, basal bodies and their associated structures are seen duplicated, the Golgikinesis occurs (Figs. 14–15). Then, the sets of basal bodies gradually move apart in opposite directions (Fig. 19C–E). As a consequence, all other skeletal appendages located at the anterior region of the cell also migrate, and each Golgi also follows this migration (Fig. 19F–H). The position displayed by the axostyle – anterior portion separated and tips together – indicates that the cell is in the prophase of mitosis (Fig. 19C–D). When axostyle sliding and crossing occurs, the posterior tips start to move apart indicating karyokinesis and the transition of metaphase to anaphase (Fig. 19E–G). Next, the axostyles continue to cross until they get parallel. Subsequently, due to further spindle elongation and the complete migration of basal bodies, axostyles reach alignment (Fig. 19H). At this point, one can recognize two small, teardrop-shaped cells linked by a straight connection, which characterizes phase 4 (telophase). Cytokinesis finishes when the two small daughter cells finally separate at their posterior ends. A higher magnification of *T. vaginalis* (Fig. 20) in anaphase (corresponding to Figure 19, row G) is seen after double immunolabeling using anti-α-tubulin and anti-adhesin AP51. Figures A and C show the axostyles in two different focal planes. Figure B shows the two Golgi labeled with anti-adhesin AP51. Figure D is an overlay of these images. In green, the two Golgi complexes; in blue and red, the different focal planes of the two axostyles. Each Golgi ribbon is seen following the axostyles migration, between the basal bodies and the nuclear envelope, always positioned at the anterior region of the cell. Measurements (Fig. 21) suggested an elongation of the Golgi ribbon during the course of the cell cycle. We observed that during mitosis, while the migration of each small (1.0–1.2 μm) Golgi ribbon occurs, it also elongates gradually reaching about 2.4–3.6 μm at telophase. Thus, each daughter cell presents, just after mitosis, only one Golgi ribbon that keeps growing. When its size reaches about 4.7–6.0 μm, the Golgikinesis proceeds again.


G
5


6

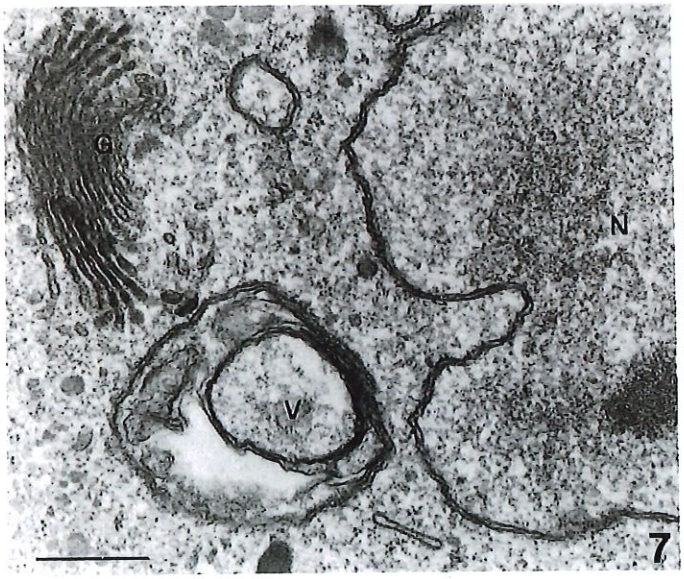
G
N
V
7

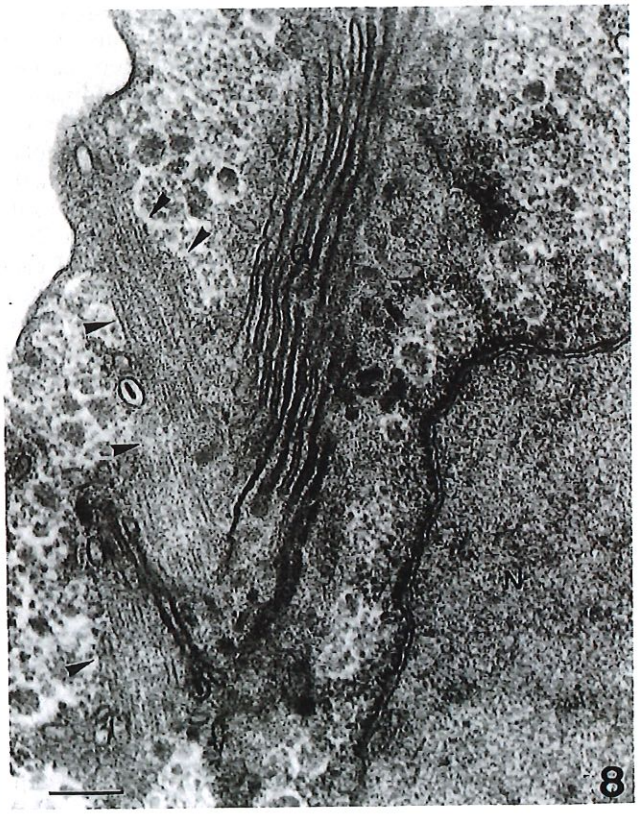
G
N
8

◀ **Fig. 5.** Close view of the Golgi complex (G) in a routine thin-section of *T. vaginalis*. Note the presence of budding coated vesicles (*arrowheads*). Bar: 0.2 μm. **Fig. 6.** Thin section of the Golgi complex (G) of *T. vaginalis* after high-pressure freezing and freeze substitution. Note a more electron-dense content of the medial Golgi cisternae, budding vesicles, and a well-preserved glycocalix (*arrowhead*). Bar: 0.2 μm. **Fig. 7.** *T. foetus* treated with 10 μM nocodazole for 12 h. The Golgi (G) is still present and does not show any sign of fragmentation. Note that the mitotic nucleus (N) presents an intact nuclear envelope. V, vacuole. Bar: 0.5 μm. **Fig. 8.** Thin section of a routine preparation of *T. foetus* showing a bundle of microtubules (*arrowheads*) interacting with the Golgi (G) and the cell cortex. N, nucleus. Bar: 0.2 μm.

Discussion

The Golgi complex of higher eukaryotic cells has been thoroughly studied, and several authors present, at least, three minimal functions that Golgi must accomplish: (*1*) receipt and sorting of membrane and soluble cargo arriving at the *cis* region from the endoplasmic reticulum; (*2*) glycosylation and processing of glycoproteins and glycolipids and (*3*) sorting of materials and membrane at *trans* face of this organelle (Mellman and Simons, 1992). Although the details of Golgi morphology vary considerably between different cell types, a four compartment subdivision (*cis, medial, trans* and *TGN*) is also consistent with the functional organization of the Golgi in *T. vaginalis* and *T. foetus*.

Golgi structure

Routine thin sections of trichomonads cells do not give all the information about the role and the exact number and distribution of the Golgi cisternae and their contents. Cryofixation vastly improves the preservation of cell structure, giving the user confidence that the images produced are a close representation of the living cell. This has allowed a better preservation of all cell organelles, Golgi and related structures included. Thus, we performed our studies using complementary techniques such as quick- or high-pressure freezing of living cells, freeze substitution and immunocytochemistry. These methodologies allowed us to confirm our findings obtained using routine techniques. Among the few differences observed when fast-freezing was used are the higher density of medial Golgi

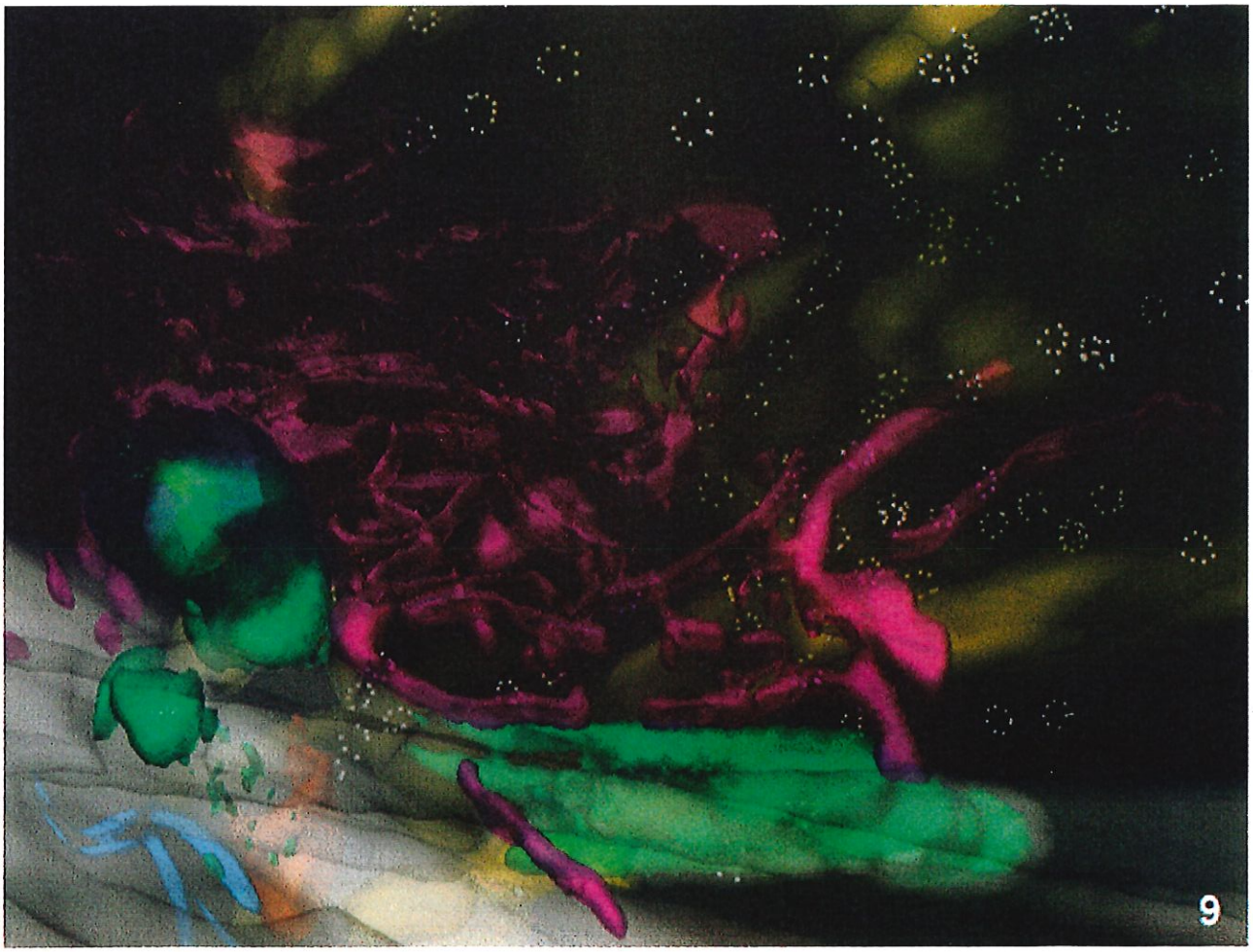

Fig. 9. SYNU 3D computer model showing a top view of one pole of *T. foetus* during prometaphase in mitosis. The Golgi apparatus (*pink*) is located between the nuclear compartment (*yellow*) and the emergence of the basal bodies/recurrent flagellum (*green*). Scattered polyribosomes (*white circular particles*), a portion of the cell membrane (*gray*), part of the sigmoidal filaments (*blue*), and also some of the microtubule-organizing centers (*orange*) are shown.

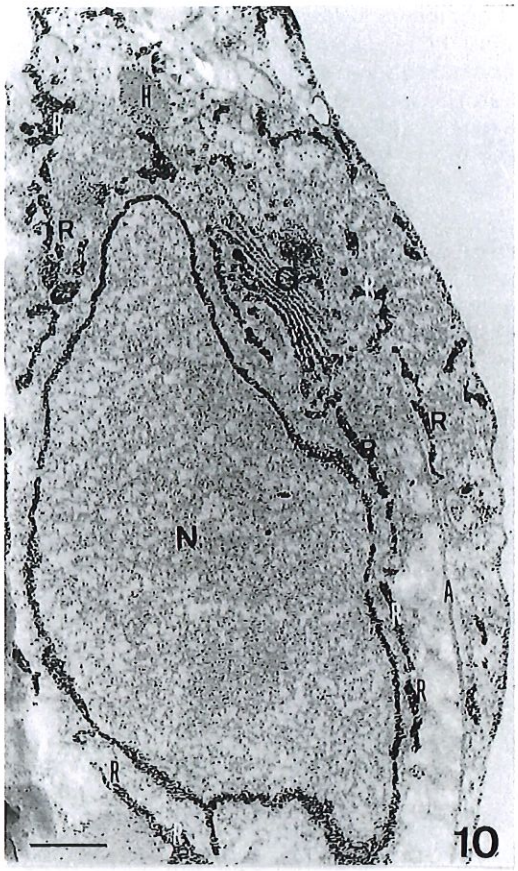
H
R
R
G
R
R
N
A
R
R
R
10

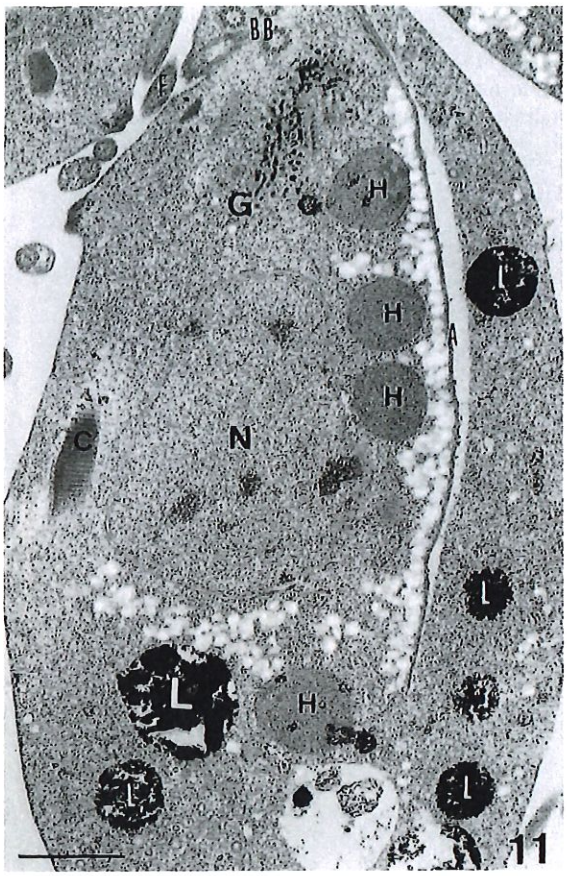
BB
G
H
H
H
L
A
C
N
L
L
H
L
L
11

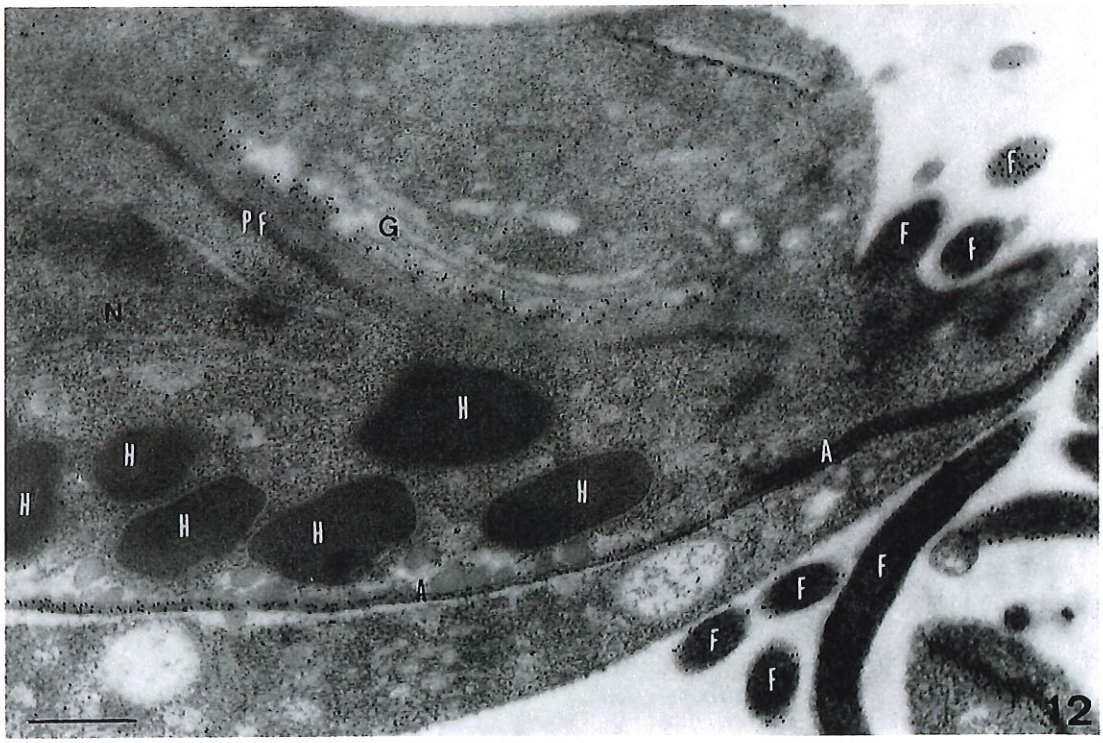
F
PF
G
F
F
N
H
H
A
H
H
H
H
A
F
F
F
F
F
12

◀ **Fig. 10.** *T. foetus* after cytochemistry for Ca^{++}-ATPase. An intense labeling is seen on the nuclear envelope, endoplasmic reticulum profiles (R) and in the Golgi apparatus (G), in which some cisternae are more intensely labeled than others. A, axostyle; H, hydrogenosome; N, nucleus. Bar: 0.5 μm. **Fig. 11.** *T. foetus* seen after cytochemistry for acid phosphatase. Several lysosomes are densely labeled (L) and also the Golgi complex (G). A, axostyle; BB, basal bodies; F, flagella; H, hydrogenosomes; N, nucleus. Bar: 1 μm. **Fig. 12.** *T. foetus* after immunocytochemistry for anti-glutamylated tubulin. An intense labeling is seen on the pelta-axostyle system (A), flagella (F), and in the Golgi region (G). H, hydrogenosomes; N, nucleus; PF, parabasal filament. Bar: 0.5 μm.

cisternae contents, the observation of thin fibrils connecting each stack and a better visualization of the glycocalix.

We only found two Golgi when cells demonstrate signs of the synthesis phase or mitosis, i.e., duplicated cytoskeletal structures, such as the axostyle and pelta, as we have previously demonstrated (Ribeiro et al., 2000). By freeze-fracture, we were able to see that *T. foetus* Golgi is a highly fenestrated structure at the most proximal and most distal cisternae. In a previous study (Benchimol et al., 1993) quick-freezing and freeze-etching revealed 2 nm wide filamentous structures in the luminal space of the Golgi complex, connecting the two faces of each cisternae.

Golgi and secretion

Receptor-ligand-type interactions are involved between trichomonads and epithelial cells (Arroyo et al., 1993). Four trichomonads surface proteins, referred to as adhesins, were identified in *T. vaginalis* as mediating cytoadherence, and synthesis of the four adhesins was coordinately up-regulated by binding to epithelial cells (Arroyo et al., 1993) and by iron (Lehker et al., 1991). *T. foetus* cytoadherence also occurs and promotes morphologic transformation (Nielsen and Nielsen, 1975). All these events involve protein synthesis, and consequently the cell secretory pathway. We were able to find labeling for adhesins in Golgi, vesicles and cell surface, using immunogold technique (Alderete et al., 2000). In the present study we used anti-adhesin antibodies in order to follow the Golgi, and the secretory pathway along the course of the cell cycle in trichomonads. In higher eukaryotic cells the secretion activity is altered during mitosis, the traffic out the endoplasmic reticulum is blocked and the exocytosis stops as direct consequence of the Golgi fragmentation (Alberts et al., 1994). In trichomonads, as the Golgi structure is maintained during mitosis, and adhesins are found in the secretory pathway, it seems that secretion and exocytosis are continuous during the whole cell cycle. Further studies are necessary to better clarify this question.

Association of the Golgi complex with other cell structures

Parabasal filaments. Previous studies have proposed that there are two parabasal filaments (PF) in trichomonads, and each one is known to support each dictyosome of the Golgi apparatus, the whole forming the so-called parabasal apparatus from where the phylum Parabasalia derives its name (Brugerolle and Viscogliosi, 1994; Honigberg and Brugerolle, 1990). Brugerolle and Viscogliosi (1994) labeled the parabasal fibers using monoclonal antibodies. These authors showed that in *T. foetus* there is a major parabasal fiber supporting a dictyosome and a minor one very close to the major fiber. In the present study we have shown, for the first time, a structural connection between the first Golgi cisternae and this periodic structure. We found that the *cis*-most region of the Golgi complex is always associated with the parabasal filaments and is also in close proximity with the endoplasmic reticulum. Thin fibrils are seen connecting the first Golgi cisternae and the parabasal filament only when fast-freezing methods were used suggesting the sensitivity of these fibrils to chemical fixatives. Studies are necessary to identify these proteins. Nevertheless, this physical connection is important since it provides a means by which the organelle remains interconnected to the basal bodies from where the parabasal filaments emerge. Keeping in mind this connection, it helps to understand why the Golgi migration follows migration of the basal bodies and flagella during mitosis (Zuo et al., 1999; Ribeiro et al., 2000). It is interesting that in other protists, such as the flagellated *Ochromonas,* the Golgi complex remains supported by a striated fiber which originates in the basal body complex. Interestingly, during the *Ochromonas* division, not only the Golgi but also the mitochondria are linked to basal bodies by connectors, and they move as a single unit to the opposite poles together with the separation of the basal bodies and flagella during the open mitosis phases (Bouck and Brown, 1973; Mignot, 1996; Chapman et al., 2000).

Endoplasmic reticulum. ZIO reaction and Ca^{++}-ATPase were found in both endoplasmic reticulum and Golgi, suggesting similarities between these structures. Maillet (1962) introduced the zinc iodide-osmium tetroxide technique, and the reaction product has been shown in some cellular structures such as synaptic vesicles, mitochondria, endoplasmic reticulum and Golgi complex. However, the cellular substances that interact with this chemical compound are not yet well established (review by Pellegrino de Iraldi (1977)). Benchimol and DeSouza (1985) previously used this technique to analyze the distribution of the endoplasmic reticulum-Golgi complex in *T. foetus.* In the present work, we have used this reaction in order to study the ER-Golgi during the division process, since a deposit of electron-dense material occurs in the lumen of these membranous systems. The nuclear pores and the Golgi fenestrae could be easily identified, appearing as a region where no deposit of electron-dense material occurs. The technique allowed a good view of the Golgi, and confirms the observations obtained by other techniques.

Cytoskeleton. When cells were fixed by high-pressure freezing or slam-freezing followed by freeze substitution, it was possible to visualize microtubules connecting the Golgi with the cell cortex. With the same procedures, the Golgi medial cisternae were found to be more electron-dense and presented a higher content. Using immunocytochemistry some of the Golgi cisternae were labeled with anti-glutamylated tubulin, suggesting the presence of microtubules or tubulin. In mammalian cells, the Golgi complex breaks down during mitosis. It is also perturbed by nocodazole treatment, allowing enzymes to accumulate in pre-Golgi intermediates (Lippincott-Schwartz and Zaal, 2000), suggesting a role of microtubules in the organization of the Golgi apparatus (Kreis, 1990). We have shown that agents (such as nocodazole) that normally alter the distribution of interphase microtubules and fragment the Golgi in other cells, do not appear to have any effect on the Golgi in trichomonads, suggesting its different composition. A possible explanation could be that, in trichomonads, the Golgi would interact with a different tubulin isoform or microtubule-associated proteins.

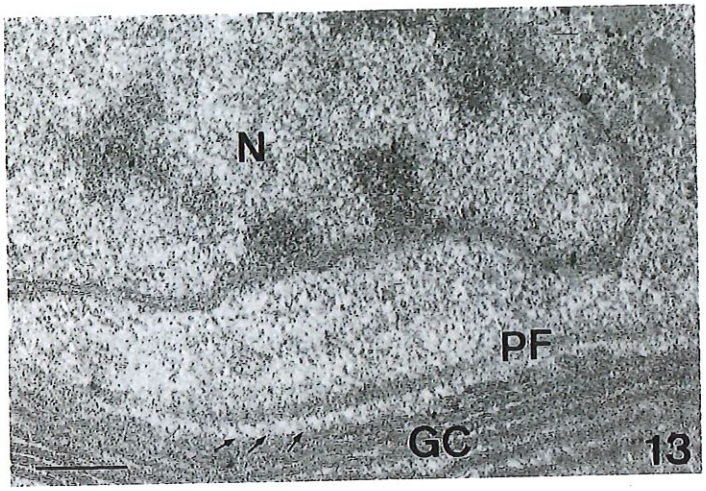
N
PF
GC
13

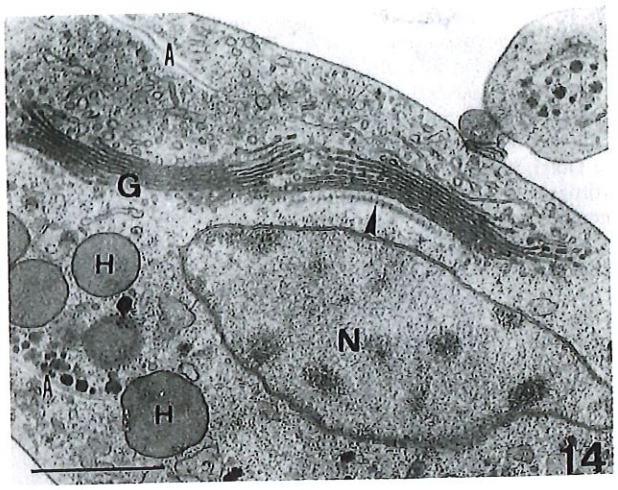
A
G
H
N
A
H
14

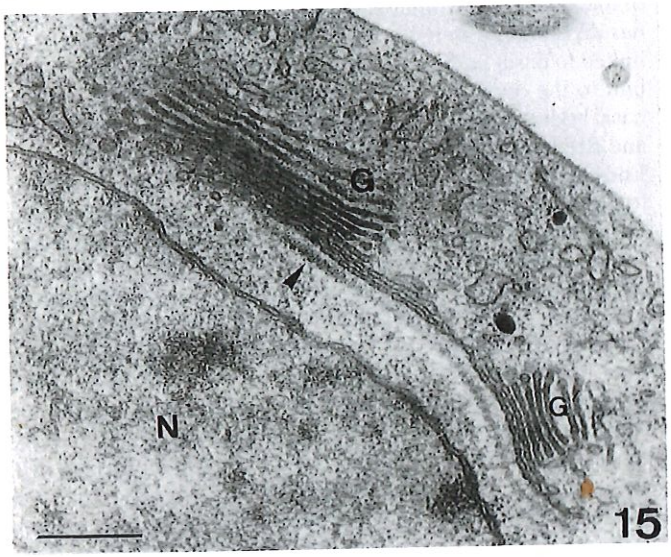
G
N
G
15

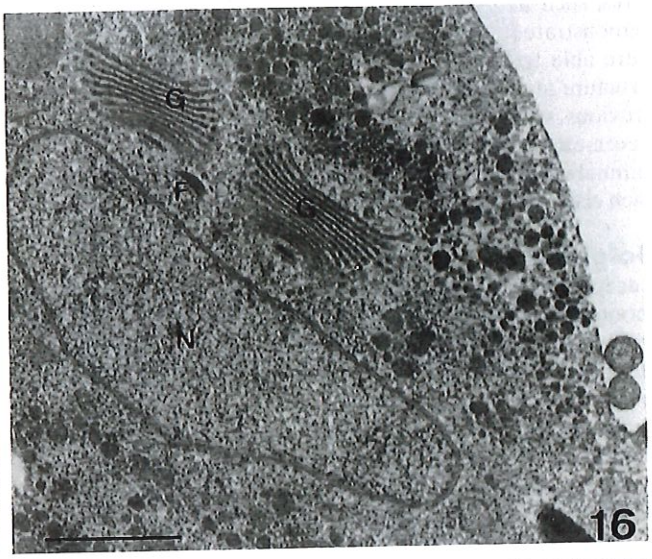
G
P
N
16

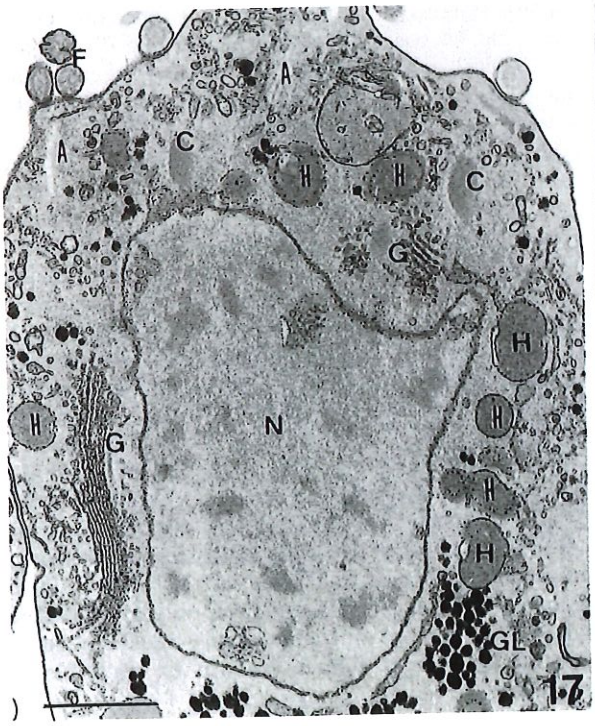
F
A
A
C
H
H
C
G
H
H
G
N
H
H
GL
17


G
N
G
N
18

◀ **Fig. 13.** Routine thin section of *T. foetus* where a parabasal filament (PF) is seen connected to the first cisternae of the Golgi complex (GC) by thin filaments (*small arrows*). N, nucleus. Bar: 0.2 μm. **Fig. 14.** Image of *T. foetus* showing the Golgi (G) in Golgikinesis. **Fig. 15.** In Figures 14 and 15 a well-developed Golgi with its parabasal filament (*arrowhead*) appears to undergo fission. These cells are in a pre-mitotic phase. A, axostyle; H, hydrogenosomes; N, nucleus. **Fig. 16.** Figure 16 shows two small Golgi complexes (G) but the cell is still in a pre-mitotic phase. N, nucleus. Bars: 1 μm (Fig. 14, 16), 0.5 μm (Fig. 15). **Fig. 17.** *T. foetus* in prophase is shown after Thiéry's technique, which reveals carbohydrates. Note that two axostyles (A), two costa (C), two Golgi (G), and a nucleus (N) are seen. All of these structures do not fragment during the mitotic process. GL, glycogen granules; H, hydrogenosomes. Bar: 1 μm. **Fig. 18.** *T. foetus* after ZIO technique, which labels Golgi membranes (G), endoplasmic reticulum and the nuclear envelope. This cell is in division. Two Golgi and a nucleus in process of karyokinesis are seen. Note the pore complexes (*arrowheads*). Bar: 0.2 μm.

Lysosomes. Cells submitted to cytochemistry for acid phosphatase showed intense labeling in several cisternae of the Golgi, associated vesicles and lysosomes. Budding vesicles presented intense reaction, suggesting that lysosomes in trichomonads seem to be formed by the same pathway as that of higher eukaryotic cells. Brugerolle (1971) and Garcia-Tamayo et al. (1978) observed that after cytochemistry for acid phosphatase, the Golgi complex as well some vesicles adjacent to this structure presented positive reaction.

Golgi functions

Ca^{++} regulation. The calcium pools generated within the endoplasmic reticulum, Golgi complex and other organelles are believed to participate in the regulation of a variety of cell functions (Pezzati et al., 1997). It has been shown that, in trichomonads, calcium storage takes places in the hydrogenosomes and endoplasmic reticulum, and more recently in the Golgi complex (Almeida et al., submitted). The observation of a Ca^{++}-ATPase in the Golgi cisternae supports these findings. Another possibility, raised by the use of cryofixation, is that the denser content of the Golgi and dilations that we observed in the medial stacks could represent sites of ion accumulation as observed in the endoplasmic reticulum. We have shown recently that cryotechniques vastly improves preservation of cell morphology and ion immobilization when compared to chemical fixation carried out in routine TEM preparations (Ribeiro et al., 2001).

Recently, using isolated membranes, we demonstrated a striking participation of the Golgi of *T. foetus* in the Ca^{2+} uptake and the presence of a Ca^{++}-ATPase in the organelle (Almeida et al., submitted). In the present study we demonstrate by cytochemistry a Ca^{++}-ATPase in the endoplasmic reticulum and Golgi complex in trichomonads. In addition, similar results were obtained using the osmium-pyroantimonate technique (Almeida et al., submitted). According to Motzko and Ruthman (1990), the Golgi complex assumes a predominant role in calcium sequestration during meiosis of the insect *Dysdercus intermedius*. Pezzati et al. (1997) showed by high-resolution calcium mapping in neurosecretory cells that the calcium pools are segregated within the endoplasmic reticulum, Golgi complex, and other organelles. We intend to apply further this methodology in the trichomonads cells.

Protein processing. Previous studies in *T. foetus* using periodic acid-thiosemicarbazide-silver proteinate showed positive reaction in the Golgi membranes, indicating the presence of carbohydrates (Benchimol et al., 1982). However, no attention was paid to the Golgi cisternae contents. In the present study, we demonstrated using fast-freezing and freeze-substitution techniques that there are different electron densities through the Golgi cisternae in *T. foetus*. It probably could be a reflection of different contents in Golgi stacks. On the other hand, using gold-labeled lectins, we were able to show the presence of different sugars along the Golgi stacks (Benchimol and Bernardino, 2001), suggesting that one function of the Golgi in *T. foetus* would be glycosylation, as in higher eukaryotic cells.

Golgi biogenesis

During interphase, there is only one Golgi ribbon in *T. foetus* and *T. vaginalis*, whereas at the onset of mitosis two Golgi ribbons are found, always close to the nucleus and following it during all phases of the division process. Some authors (Honigberg and Brugerolle, 1990) believed that *T. vaginalis* presents two Golgi complexes. In our opinion, the analyses made by these authors were performed with cells in the process of division or in S/G2 interphasic cells. In the present study we demonstrate that the Golgi does not fragment during mitosis, but rather it seems to elongate; and once it has at least duplicated in size, it is separated in two, in a process herein named as Golgikinesis. This process occurs during interphase as a pre-mitotic event. A quantitative study was performed and clearly showed that immediately after Golgikinesis two small Golgi ribbons are found. Each Golgi gradually elongates during the course of the mitotic process and also during the interphase until Golgikinesis is re-initiated.

Several organisms such as dinoflagelates, trichomonads, *Drosophila* embryos, and insects (during gamete formation) present closed or semi-opened mitosis and are known to display permanent Golgi complexes along all mitotic phases (Barlow and Triemer, 1988; Fritz and Triemer, 1983; Camp et al., 1974, Motzko and Ruthman, 1990; Stanley et al., 1997). On the other hand, in joenids which are termite hindgut flagellates belonging to the phylum Parabasalia, the Golgi complexes are reported to disassemble during the beginning of mitosis and then to be rebuilt in telophase (Hollande and Valentin, 1969). It is important to point out that, in this case, the parabasal filaments and other constituents of the cytoskeleton as the axostyle and mastigont system (flagella and appended structures) undergo the same process of fragmentation and reconstitution during mitosis. This view of disassembly and reformation of skeletal structures along mitosis in trichomonads is also held by Brugerolle (1975) despite of the fact that he did not report observations on the Golgi complex behavior.

Other protists, such as Euglenes, present dictyokinesis, in which a Golgi division occurs through a constriction of saccules, which have grown longer (Mignot, 1965). In plants, it is well known that the Golgi stacks remain intact, analogous to the budding yeast which undergoes a closed nuclear division (Stanley et al., 1997). However, the exact behavior of the persistent Golgi complexes during mitosis is not well known as compared to the more general scheme of the fragmenting Golgi typical of higher eukaryotes.

The current view in open mitosis of higher eukaryotes supports the idea that part of the Golgi complex breaks up into a set of smaller fragments and vesicles whereas the remnants of it are redistributed to the endoplasmic reticulum (Zaal et al., 1999; Terasaki, 2000; Nelson, 2000).

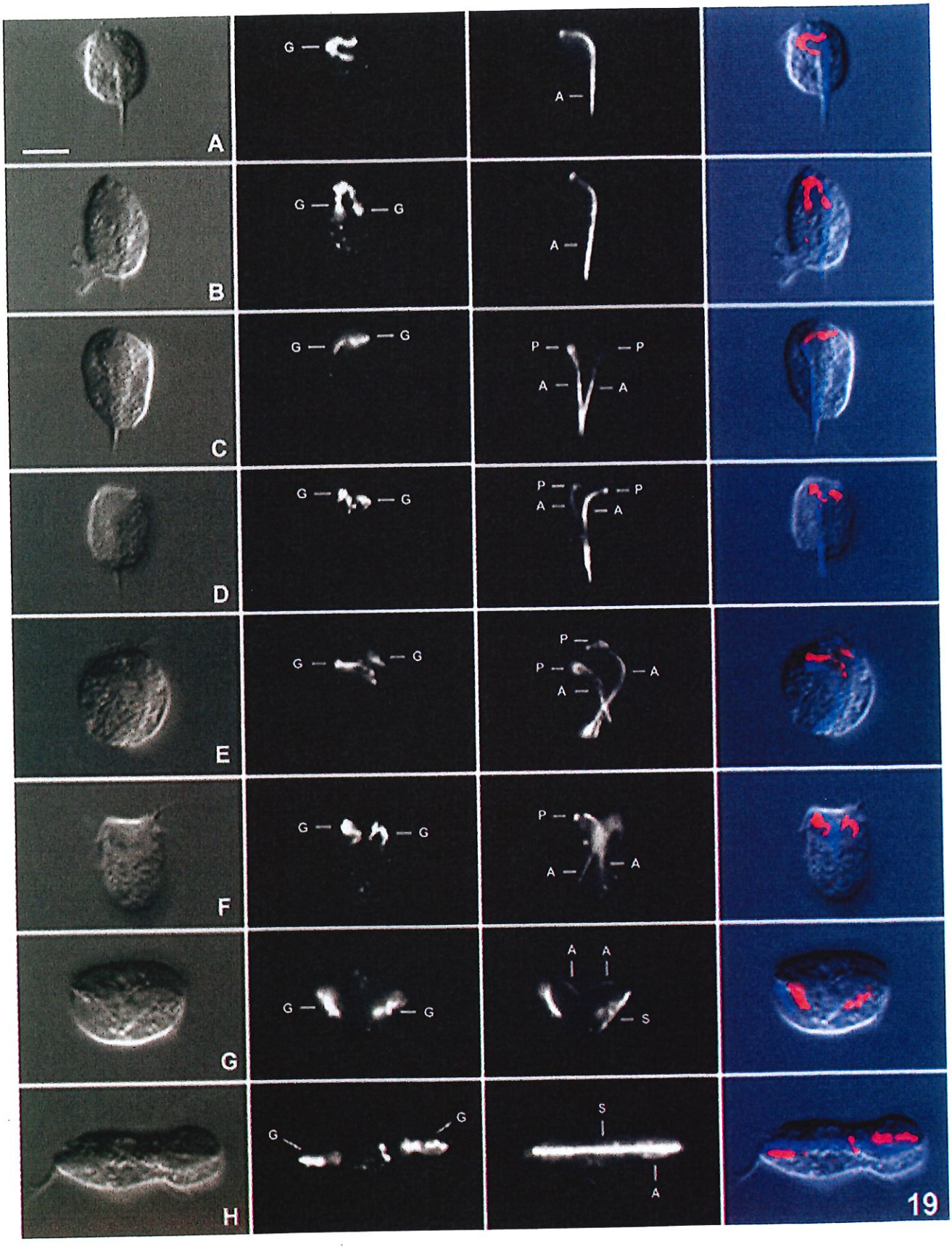
A
G
A
B
G
G
A
C
G
G
P
P
A
A
D
G
G
P
P
A
A
E
G
G
P
P
A
A
F
G
G
P
A
A
G
G
G
A
A
S
H
G
G
S
A
19

◀ **Fig. 19.** *T. vaginalis* during morphogenesis from interphase (**A**) through pre-mitosis (**B**) and mitosis (**C–H**). The double-label staining of α-tubulin (*blue*) and anti-adhesin AP65 (*red*), shows the correlation of number and position of the axostyle and the Golgi. The *first column* shows the DIC images; the *second column* shows the corresponding anti-AP65 labeling; the *third column* shows the α-tubulin fluorescence; and, finally, the *fourth column* shows the overlay of the other images. **A**: *T. vaginalis* in interphase (G1), where a single Golgi copy (G) is seen, as well as one axostyle (A) and one pelta (P). **B**: the cell is in interphase (S/G2) and presents an axostyle (A) but already two Golgi ribbons are seen side-by-side. **C**: the cell in mitosis (prophase) is larger and shows two aligned Golgi (G), the axostyle (A) and the pelta (P) already duplicated. **D** and **E**: mitotic cells in phase 2 (metaphase): the cell progressively assumes a triangular shape since the axostyles are separated at the anterior region whereas their tips are together. In phase 3 (anaphase, **F** and **G**) the axostyle (A) tips are separated and each Golgi migrates. **H**: Mitosis in phase 4 (telophase) where the daughter cells are joined only by their posterior regions. The Golgi (G) are in opposite positions whereas the axostyles are aligned. Note the presence of the spindle (S), which is labeled in the last phases of division. Bar: 4 μm.

The endomembrane system, specifically the Golgi apparatus or associated vesicles, has been reported at or close to the poles in many organisms investigated (Camp et al., 1974; Barlow and Triemer, 1988). In some cases, a region of the cytoplasm, referred to as "archoplasmic sphere", that is devoid of organelles and is enclosed by the Golgi apparatus, is thought to organize the spindle (Cachon and Cachon, 1977; Soyer, 1972, 1971). Curiously, in *Ochromonas*, the periodic fiber which supports the Golgi and has its origin in the basal bodies was clearly shown to act as a microtubule-organizing center (MTOC) orienting spindle pole formation during open mitosis (Bouck and Brown, 1973).

According to a recent report (Margulis et al., 2000), after trichomonads cell division, one daughter cell retains the Golgi and the other one has to synthesize a totally new organelle as occurs with the axostyle. Our findings are in disagreement with this author's view. We observed that in *T. foetus* and *T. vaginalis* mitosis, the Golgi complex, parabasal filaments, flagella/basal bodies, MTOC, pelta-axostyle complex and nuclear genome replicate in a pre-mitosis phase and undergo segregation along the closed mitosis phases as a unit in a similar way to the *Ochromonas* process (Ribeiro et al., 2000). The dynamics of the extranuclear spindle and flagella seem to drive the separation of the duplicated cytoplasts (Ribeiro et al., 2000, Benchimol et al., 2000) and consequently the organelles associated with the skeletal structures, such as the Golgi. We claim that in trichomonads mitosis, the cytoskeletal elements remain stable and are combined to promote nuclear and cell division (Ribeiro et al., 2000). In this regard, skeleton-associated organelles, such as the Golgi, follow cytoskeletal division during synthesis phase and during migration, elongation and separation of daughter cells during mitosis, thus holding a new view on the behavior of these cell structures during cell division.

Acknowledgements. The authors wish to thank Dr. Wanderley de Souza for critical reading the manuscript and Dr. Mark H. Ellisman for the use of facilities of National Center for Microscopy (Grant NIHRR0450). This work was supported by CNPq (Conselho Nacional de Desenvolvimento Científico e Tecnológico), PRONEX (Programa de Núcleos de Excelência), FAPERJ (Fundação Carlos Chagas Filho de Amparo à Pesquisa do Estado do Rio de Janeiro), CAPES (Coordenação de Aperfeiçoamento de Pessoal de Nível Superior) and AUSU (Associação Universitária Santa Úrsula).

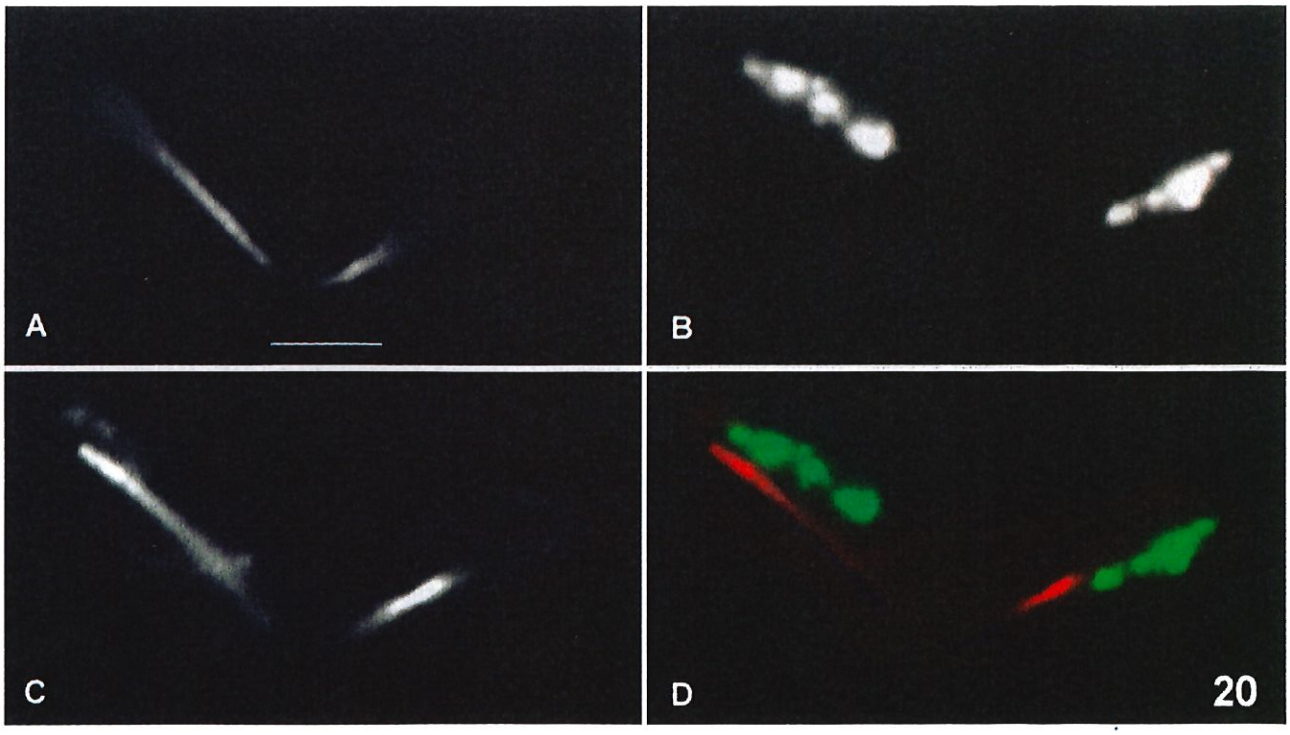

Fig. 20. A higher magnification of *T. vaginalis* in anaphase (corresponding to Figure 19G) after double immunolabeling with anti-α-tubulin and anti-adhesin 2 (AP51). **A, C**: axostyles, with anti-α-tubulin labeling, in two different focal planes. **B**: the two Golgi labeled with anti-adhesin 2. **D**: overlay of the images. In *green*, the two Golgi complexes; in *blue* and *red*, the different focal planes of the two axostyles. Bar: 2 μm.

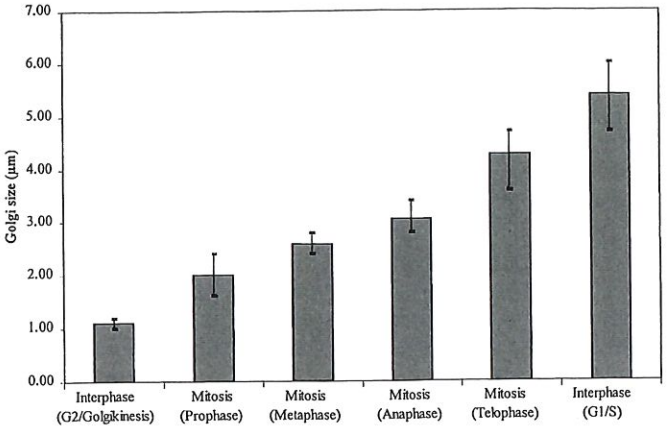

Fig. 21. Size of the Golgi during the cell cycle phases. One hundred cells were taken from different phases in mitosis and interphase. The Golgi ribbon size was measured and the phase was established according to parameters published previously (Ribeiro et al., 2000). Note that the Golgi gradually grows during the course of the cell cycle.

References

Alberts, B., Bray, D., Lewis, J., Raff, M., Roberts, K., Watson, J. D. (1994): Molecular Biology of the Cell. Garland Publishing, Inc. New York.

Alderete, J. F., Bernardino, M. V., Benchimol, M. (2000): Iron regulates compartmentalization of the *Trichomonas vaginalis* cytadhesins. Mol. Biol. Cell **11**, 485a.

Alderete, J. F., Garza, G. E. (1988): Identification and properties of *Trichomonas vaginalis* proteins involved in cytoadherence. Infect. Immun. **56**, 28–33.

Arroyo, R., Engbring, J., Alderete, J. F. (1992): Molecular basis of host epithelial recognition by *Trichomonas vaginalis*. Mol. Microbiol. **6**, 853–862.

Arroyo, R., Gonzalez-Robles, A., Martinez-Palomo, A., Alderete, J. F. (1993): Signalling of *Trichomonas vaginalis* for amoeboid transformation and adhesion synthesis follows cytoadherence. Mol. Microbiol. **7**, 299–309.

Barlow, S. B., Triemer, R. E. (1988): The mitotic apparatus in the dinoflagellate *Amphidinium carterae*. Protoplasma **145**, 16–26.

Benchimol, M., Bernardino, M. V. (2001): Ultrastructural localization of glycoconjugates in *Tritrichomonas foetus*. Parasitol. Res. (in press).

Benchimol, M., DeSouza, W. (1985): *Tritrichomonas foetus*: cytochemical visualization of the endoplasmic reticulum-Golgi complex and lipids. Exp. Parasitol. **59**, 51–58.

Benchimol, M., Diniz, J. A. P., Ribeiro, K. (2000) The fine structure of the axostyle and its associations with organelles in trichomonads. Tissue Cell **32**, 178–187.

Benchimol, M., Elias, C. A., DeSouza, W. (1982): *Tritrichomonas foetus*: ultrastructural localization of basic proteins and carbohydrates. Exp. Parasitol. **54**, 135–144.

Benchimol, M., Kachar, B., DeSouza, W. (1993): The structural organization of the pathogenic protozoan *Tritrichomonas foetus* as seen in replicas of quick frozen, freeze-fractured and deep etched cells. Biol. Cell **77**, 289–295.

Bouck, B. G., Brown, D. L. (1973): Microtubule biogenesis and cell shape in *Ochromonas*. I. the distribution of cytoplasmic mitotic microtubules. J. Cell Biol. **56**, 340–359.

Brugerolle, G. (1971): Mise en évidence du processus d'endocytose et des structures lysosomiques chez *Trichomonas vaginalis*. C.R. Acad. Sc. Paris. **272**, 2553–2560.

Brugerolle, G. (1975): Étude de la cryptopleuromitose et de la morphogenèse de division chez *Trichomonas vaginalis* et plusieurs genres de Trichomonadines primitives. Protistologica **4**, 457–468.

Brugerolle, G., Viscogliosi, E. (1994): Organization and composition of the striated roots supporting the Golgi apparatus, the so-called parabasal apparatus, in parabasalid flagellates. Biol. Cell **81**, 277–285.

Cachon, J., Cachon. M. (1977): Observation on the mitosis and on the chromosome evolution during the life cycle of *Oodinium*, a parasitic dinoflagellate. Chromosoma **60**, 237–251.

Camp, R. R., Mattern, F. T. C., Honigberg, B. M. (1974): Study of *Dieantamoeba fragilis* Jepps & Dobell I. Electronmicroscopic observation of the binucleate stages II. Taxonomic position and revision of the genus. J. Protozool. **21**, 69–82.

Cavalier-Smith. T., Chao, E. E. (1996): Molecular phylogeny of the free-living archeozoan *Trepomonas agilis* and the nature of the first eukaryote. J. Mol. Evol. **43**, 551–562.

Chapman, M. J., Dolan, M. F., Margulis, L. (2000): Centrioles and kinetosomes: form, function and evolution. Quart. Rev. Biol. **75**, 409–429.

Diamond, L. S. (1957): The establishment of various trichomonads of animals and man in axenic cultures. J. Parasitol. **43**, 488–490.

Embley, T. M., Hirt, R. P. (1998): Early branching eukaryotes? Curr. Opin. Genet. Dev. **8**, 624–629.

Fritz, L., Triemer, R. E. (1983): An ultrastructural study of mitosis in a marine dinoflagellate: *Prorocentrum minimum*. J. Protozool. **30**, 437–444.

Garcia-Tamayo, J., Nunes-Montiel, J. T., Garcia, H. P. (1978): An electron microscopy investigation on the pathogenesis of human vaginal trichomoniasis. Acta Cytol. **22**, 447–455.

Hessler, D., Young, S. J., Carragher, B. A., Martone, M., Hinshaw, J. E., Milligan, R. A., Masliah, E., Whittaker, M., Lamont, S., Ellisman, L. H. (1992): SYNU: software for visualization of 3-D biological structures. Microscopy: the key research tool, March, 73–82.

Hollande, A., Valentin, J. (1969): Appareil de Golgi, pynocytose, lysosomes, mitochondries, bactéries symbiontiques, atractophores et pleuromitose chez les hypermastigines du genre *Joenia*. Affinités entre Joenides et Trichomonadines. Protistologica **5**, 39–86.

Honigberg, M. B., Brugerolle, G. (1990): Structure. In: B. M. Honigberg (ed.): Trichomonads Parasitic in Human. Springer-Verlag, pp. 5–35.

Kreis, T. E. (1990): Role of microtubules in the organization of the Golgi apparatus. Cell Motil. Cytoskeleton **15**, 67–70.

Kurland, C. G., Andersson, S. G. E. (1999): Origins of mitochondria and hydrogenosomes. Curr. Opin. Microbiol. **2**, 535–541.

Lehker, M. W., Arroyo, R., Alderete, J. F. (1991): The regulation by iron of the synthesis of adhesins and cytoadherence levels in the protozoan *Trichomonas vaginalis*. J. Exp. Med. **174**, 311–318.

Leipe, D. D., Gunderson, H. J., Nerad, A. T., Sogin, L. M. (1993): Small subunit ribosomal RNA$^+$ of *Hexamita inflata* and the quest for the first eukaryotic tree. Mol. Biochem. Parasitol. **59**, 41–48.

Lippincott-Schwartz, J., Zaal, K. J. M. (2000): Cell cycle maintenance and biogenesis of the Golgi complex. Histochem. Cell Biol. **114**, 93–103.

Maillet, M. (1962): La technique de Champy a l'osmium ioduré de zinc. Trabahos do Instituto Cajal de Investigaciones Biologicas **54**, 1–36.

Margulis, L., Dolan, F. M., Guerrero, R. (2000): The chimeric eukaryote: origin of the nucleus from the karyomastigont in amitochondriate protists. Proc. Natl. Acad. Sci. USA **97**, 6954–6959.

Mellman, I., Simons, K. (1992): The Golgi complex: in vitro veritas? Cell **68**, 829–840.

Mignot, J. P. (1965): Étude ultrastructurale des euglèniens: II. A, dictyosomes et dictyocinèse chez *Distigma proteus* Ehrbbg B, mastigoonèmes chez *Anisonema costatum* Christen. Protistologica **1**, 17–24.

Mignot, J. P. (1996): The centrosomal big bang: From a unique central organelle towards a constellation of MTOCs. Biol. Cell **86**, 81–91.

Morgado, J. A., DeSouza, W. (1998): Biochemical characterization of the Golgi-complex proteins of *Tritrichomonas foetus*. Parasitol. Res. **84**, 760–762.

Motzko, D., Ruthman, A. (1990): Spindle membranes and calcium sequestration during meiosis of *Dysdercus intermedius* (Heteroptera). Chromosoma **99**, 212–222.

Müller, M. (1993): The hydrogenosome. J. Gen. Microbiol. **139**, 2879–2889.

Müller, M. (1997): Evolutionary origins of trichomonad hydrogenosomes. Parasitol. Today **13**, 166–167.

Nelson, J. W. (2000): W(h)ither the Golgi during mitosis? J. Cell Biol. **149**, 243–248.

Nielsen, M. H. Nielsen, R. (1975): Electron microscopy of *Trichomonas vaginalis* Donné. Interaction with vaginal epithelial in human trichomoniasis. Acta Pathol. Microbiol. Scand. Sect. B. **83**, 305–320.

Pellegrino de Iraldi, A. (1977): Significance of the Maillet method (ZIO) for cytochemical studies of structures. Experientia **33**, 1–10.

Pezzati, R., Bossi, M., Podini, P., Meldolesi, J., Grohovaz, F. (1997): High-resolution calcium mapping of the endoplasmic reticulum-Golgi-exocytic membrane system. Mol. Biol. Cell **8**, 1501–1512.

Pozzan, T., Rosario, R., Volpe, P., Meldolesi, J. (1994): Molecular and cellular physiology of intracellular calcium stores. Physiol. Rev. **74**, 595–635.

Queiroz, R. C. B., Santos, L. M. S., Benchimol, M., DeSouza, W. (1991): Cytochemical localization of enzyme markers in *Tritrichomonas foetus*. Parasitol. Res. **77**, 561–566.

Reinecke, M., Walther, C. (1978): Aspects of turnover and biogenesis of synaptic vesicles at locust neuromuscular junction as revealed by zinc-iodide-osmium tetroxide (ZIO) reacting with intravesicular -SH groups. J. Cell Biol. **78**, 839–855.

Ribeiro, K. C., Benchimol, M., Farina, M. (2001): Contribution of cryofixation and freeze-substitution to analytical microscopy: A study of the *Tritrichomonas foetus* hydrogenosome. Microsc. Res. Tech. **53**, 87–92.

Ribeiro, K. C., Diniz, J. A. P., Benchimol, M. (2000): Contributitions of the axostyle and flagella in the division process of *Tritrichomonas foetus* and *Trichomonas vaginalis*. J. Euk. Microbiol. **47**, 481–492.

Robinson, J. M., Karnovsky, M. J. (1983): Ultrastructural localization of several phosphatases with cerium. J. Histochem. Cytochem. **31**, 1197–1208.

Soyer, M. O. (1971): Structure du noyau des *Blastodinium* (Dinoflagellés parasites). Division et condensation chromatique. Chromosoma **33**, 70–114.

Soyer, M. O. (1972): Les ultrastructures nucléaire de la Noctilique (Dinoflagellé libre) au cours de la sporogénèse. Chromosoma **39**, 419–441.

Stanley, H., Botas, J., Malhotra, V. (1997): The mechanism of Golgi segregation during mitosis is cell type-specific. Proc. Natl. Acad. Sci. USA **94**, 14467–14470.

Terasaki, M. (2000): Dynamics of the endoplasmic reticulum and Golgi apparatus during early sea urchin development. Mol. Biol. Cell **11**, 897–914.

Viscogliosi, E., Brugerolle, G. (1993): Cytoskeleton in trichomonads. Eur. J. Protistol. **29**, 160–170.

Young., J. S., Suzanne, M. R., Philip, M. G., Kinnamon, C. J. (1987): Three-dimensional reconstructions from serial micrographs using the IBM PC. J. Electron Microsc. Tech. **6**, 207–217.

Zaal, K. J. M, Smith, C. L., Polishchuk, R. S., Altan, N., Cole, B., Ellenberg, J., Hirschberg, K., Presley, J. F., Roberts, T. H., Siggia, E., Phair, R. D., Lippincott-Schwartz, J. (1999): Golgi membranes are absorbed into and reemerge from the ER during mitosis. Cell **99**, 589–601.

Zuo, Y., Riley, E. D., Krieger, N. J. (1999): Flagellar duplication and migration during the *Trichomonas vaginalis* cell cycle. J. Parasitol. **85**, 203–207.